Estuarine, Coastal and Shelf Science
December 2019, Volume 231, Pages 106445 (14p.)
https://doi.org/10.1016/j.ecss.2019.106445
https://archimer.ifremer.fr/doc/00588/70049/

Hydrodynamics and SPM transport in a man-engineered tidal estuary: The Adour river (France)

Defontaine Sophie [1, *], Sous Damien [2], Morichon Denis [3], Verney Romaric [4], Monperrus Mathilde [5]

[1] CNRS / Univ. Pau & Pays Adour/ E2S UPPA, Laboratoire de Mathématiques et de leurs Applications de Pau - Fédération MIRA, UMR5142, Pau, 64000, France
[2] Université de Toulon, Aix Marseille Université, CNRS, IRD, Mediterranean Institute of Oceanography (MIO), La Garde, France
[3] Univ. Pau & Pays Adour / E2S UPPA, Laboratoire des Sciences de l'Ingénieur Appliquées à la Mécanique et au Génie Electrique (SIAME) - MIRA, EA4581, 64600, Anglet, France
[4] IFREMER, DYNECO/DHYSED, CS10070, Plouzané, 29280, France
[5] CNRS / Univ. Pau & Pays Adour/ E2S UPPA, Institut des Sciences Analytiques et de Physico-Chimie pour l'Environnement et les Matériaux - Fédération MIRA, UMR5254, 64600, Anglet, France

* Corresponding author : Sophie Defontaine, email address : sophie.defontaine@univ-pau.fr

Abstract :

The present paper reports on a series of field experiments aiming to characterise the functioning of a man-engineered strongly forced salt-wedge estuary: the lower estuary of the Adour river, France. Bottom-moored velocity measurements and surface boat surveys have been performed under low river discharge conditions, for both neap and spring tides, in order to provide a well-documented reference framework to understand the dynamics of water masses, turbulence and suspended particulate matter (SPM) transport in the lower estuary. An additional campaign has been carried out in high river discharge conditions. This first documented in-situ study of the Adour lower estuary demonstrates its variability in terms of hydrological regimes, from salt-wedge to partially mixed regimes depending on tidal and discharge conditions. Turbulent properties showed a significant response to the variations of salinity structure, with higher values when stratification is minimal. At spring tide, a tidal variation between mixing conditions on the ebb and the flood is revealed by ADCP measurements, with higher values extended up to the surface during the ebb. The link between turbulent mixing and suspended sediment concentration is straightforward during the ebb. During the flood, the suspended sediment concentration (SSC) seems related to the salt-wedge entrance re-suspension and stratification-induced turbulence damping. No stable Estuarine Turbidity Maximum (ETM) has been observed during the field experiment in the lower Adour

Highlights

► The first extensive study of the lower Adour estuary. ► The observations demonstrates a very high variability of the salinity structure, which has never been reported in the literature. ► No ETM has been identified in the present experimental conditions. ► The specific dynamics of the Adour estuary is discussed with respect to the roles of tide, river discharge and human engineering.

Keywords : Salt-wedge estuary, estuarine circulation, stratification, turbulence, suspended particles transport, Adour river

1. Introduction

Estuaries are complex transfer areas of water masses and suspended particulate matters (SPM) between ocean, land and continental waters [12]. They constitute unique habitats for a large variety of living organisms and essential nurseries for many marine species. In the overall context of climate change and growing anthropogenic pressure, a key issue of the preservation of estuarine ecosystems is to improve our knowledge of the hydro-dynamical processes controlling the dynamics and renewal of water masses in estuaries and their ability to transport, expel or retain sediments, contaminants, nutrients and living organisms.

Many studies investigated estuarine dynamics from *in-situ* measurements [16, 46, 10, 44] and/ or numerical modelling [32, 5, 41, 9]. From a physical point of view, estuaries are exchange areas between fresh brackish continental water and salty marine waters, mainly driven by river run-off, tides and wind forcing. Density gradients generated by the continental waters inter-playing with marine waters, and interactions between tides and estuarine morphology have been shown to be the major mechanisms governing the estuarine dynamics. Those mechanisms are known as : (i) gravitational circulation induced by horizontal density gradient, (ii) tidal pumping generated by an ebb-flood asymmetry, (iii) tidal straining caused by advection. The vertical salinity gradient plays also an essential role by influencing the turbulent mixing inside the water column. Note that a wide number of additional processes can also act on the estuarine dynamics and mixing, including bed morphology [16], lateral circulation [13, 14, 31, 32, 45], wind [43, 40], Earth rotation [32, 56], internal waves [54, 14, 15] and sediment load [61].

A growing interest in classifying estuaries developed along the years, in order to gain a unified view of the physics of estuaries. Different classification schemes have been proposed based on water balance, geomorphology [39], vertical salinity structure [7] or hydrodynamics [24, 56, 21]. One of the commonly used classification has been proposed by Cameron and Pritchard [7]. It is based on water column stratification, in which estuaries can be classified as salt-wedge, strongly stratified, weakly stratified or well mixed. However, the horizontal and vertical salinity gradients can show important variations in time (e.g. from neap to spring tide, or from wet to dry season) and space within a given estuary, such as stratification might not be systematically used to classify estuaries. Therefore this type of qualitative classification has been progressively forsaken, to be replaced by more quantitative methods. One recent approach has been proposed by Geyer and MacCready [21], discussing the respective contributions of tide and river flow in mixing and stratification processes. It is based on two dimensionless parameters. The former is the freshwater Froude number Fr_f [17] which express the ratio between the river flow inertia and the buoyancy due to salinity gradient. The second is the mixing parameter M which quantifies the effectiveness of tidal mixing in stratified estuaries. Geyer and MacCready proposed a mapping of various estuaries based on those two parameters, demonstrating the efficiency to discriminate different classes of estuary. For example, salt-wedge estuaries, such as the Mississippi, The Fraser and the Ebro rivers are located near the top of the Fr_f/M diagram (i.e. high values of Fr_f); while partially stratified estuaries are on the center of the diagram (e.g. James river and San Fransisco Bay) and fjords and well mixed estuaries are on the bottom part (e.g. Puget Sound). This research effort for a quantitative classification of estuaries needs to be deepened and sustained, in particular by providing relevant in-situ data from additional and contrasted case studies.

In addition to the hydrodynamic structure, a major issue of estuarine dynamics is to understand

the fate of the sediment load. Under the competing effects of turbulent suspension and gravitational settling, strong variations of Suspended Particulate Matter (SPM) concentrations are observed in both time, along the tidal cycle, and space, along the estuary [58, 18]. In the past decades, many studies, see e.g. [9, 52, 4], have revealed the presence and the mechanisms responsible for the generation of a zone of high turbidity, the so-called Estuarine Turbidity Maximum (ETM) in salt-wedge estuaries. Three major mechanisms have been highlighted in the formation of ETM. First, the estuarine circulation, due to longitudinal salinity gradient, associated with the river run-off drive a convergent SPM transport at the salt intrusion limit, that can lead to the formation of an ETM. Second, the asymmetry between the ebb and flood duration and peak velocities can also contribute to the formation of an ETM. Third, damping of turbulent mixing, due to stable stratification, can also be responsible for a sinking of particles from the upper part of the water column to the lower part. Those particles will then be advected upward by the lower layer. In addition, a recent study [23] also revealed that energetic wave conditions can influence the ETM mass by increasing the mass by a factor of 3 during mean tides. The presence or the absence of an ETM in a given estuary is a major concern when trying to understand and predict the dispersion or the retention of SPM and related biochemical issues.

A significant research effort has thus been engaged during the last two decades to perform field observations of turbulence, mixing and stratification in order to provide a basis for theoretical analysis and numerical modelling of estuarine dynamics and sediment transport [49, 50, 48, 5, 21]. The present study has been specifically designed to advance knowledge on hydrodynamics and sediment transport in a man-engineered channel-shape estuary, subjected to strong tidal and fluvial forcing, with few intertidal area and small watershed; as very few is known about such estuaries. The selected field site is the Adour river estuary, located at the bottom of the Bay of Biscay. It is a highly developed estuary with several kilometres of its downstream part completely channelised in order to secure the Bayonne harbour operations. This specific morphology is reinforced by a man-engineered reduction of the section at the last reach, in order to ease the expulsion of water and sediment. The dynamics of estuarine water masses and sediments is further affected by human interventions aiming to facilitate the navigation by dredging activities and wave protection. In addition to this very specific morphology, the Adour estuary is also subjected to important fluvial and tidal forcing, due to the location nearby the Pyrénées (heavy rainfall and snow melt freshet) and the Atlantic ocean. Despite serious economic and environmental issues related to water quality and sediment supply, very little is known about the functioning of the Adour estuary and the influence of human interventions on its internal dynamics. Most known studies have focused on the dynamics of the turbid plume and its area of influence in ocean waters [2, 11, 8, 37, 28].

The aim of our study is to gain a detailed insight on the behaviour of the current and salinity structure within the Adour river and their influence on particle matters dynamics. The present paper reports therefore on the first field experimentation conducted in the lower Adour estuary, where the marine waters play a primary role and the hydrological system remains simple enough to be monitored. The methods and instrumentation are presented in section 2. The results are detailed in section 3 and discussed in section 4. The last section is devoted to the conclusion.

2. Study site and data set

2.1. Study site

The Adour river originates in the Pyrenées mountains at an altitude of 2200 m, and flows about 300 km before pouring into the Bay of Biscay (SW of France). The catchment area is of about 17000 km^2. The annual average river discharge is of about 300 $m^3.s^{-1}$, and can reach up to more than 3 000 $m^3.s^{-1}$ during extreme flood events. The Adour river is characterised by a turbulent pulsed transport with about 75 % of annual solid flux exported within 30-40 days [38]. The estuary is exposed to a mesotidal regime, with a tidal range varying between 1 m to 4.5 m. The tidal regime is mostly composed of semi-diurnal components (M2: 1.22 m, S2: 0.42 m, N2: 0.25 m, K2: 0.12 m). The tide wave propagates until St Vincent-de-Paul (70 km upstream), and the saline intrusion limit is nearby Urt village (22 km upstream). The lower Adour river estuary (i.e. the lower 6 km), which is our zone of primary interest, is a fully man-engineered channel of 150 m to 400 m width. The main channel depth is maintained by dredging to about 10 m depth along the dock in the Bayonne harbour, to ease navigation. The estuary mouth has been straightened and channelised by embankments in order to accelerate water flow and to facilitate the sediment expulsion out of the estuary. In addition, a 700 meters long jetty has been constructed at the north side of the river mouth to protect the Bayonne harbour from swells mainly coming from the northwest sector (Fig. 1).

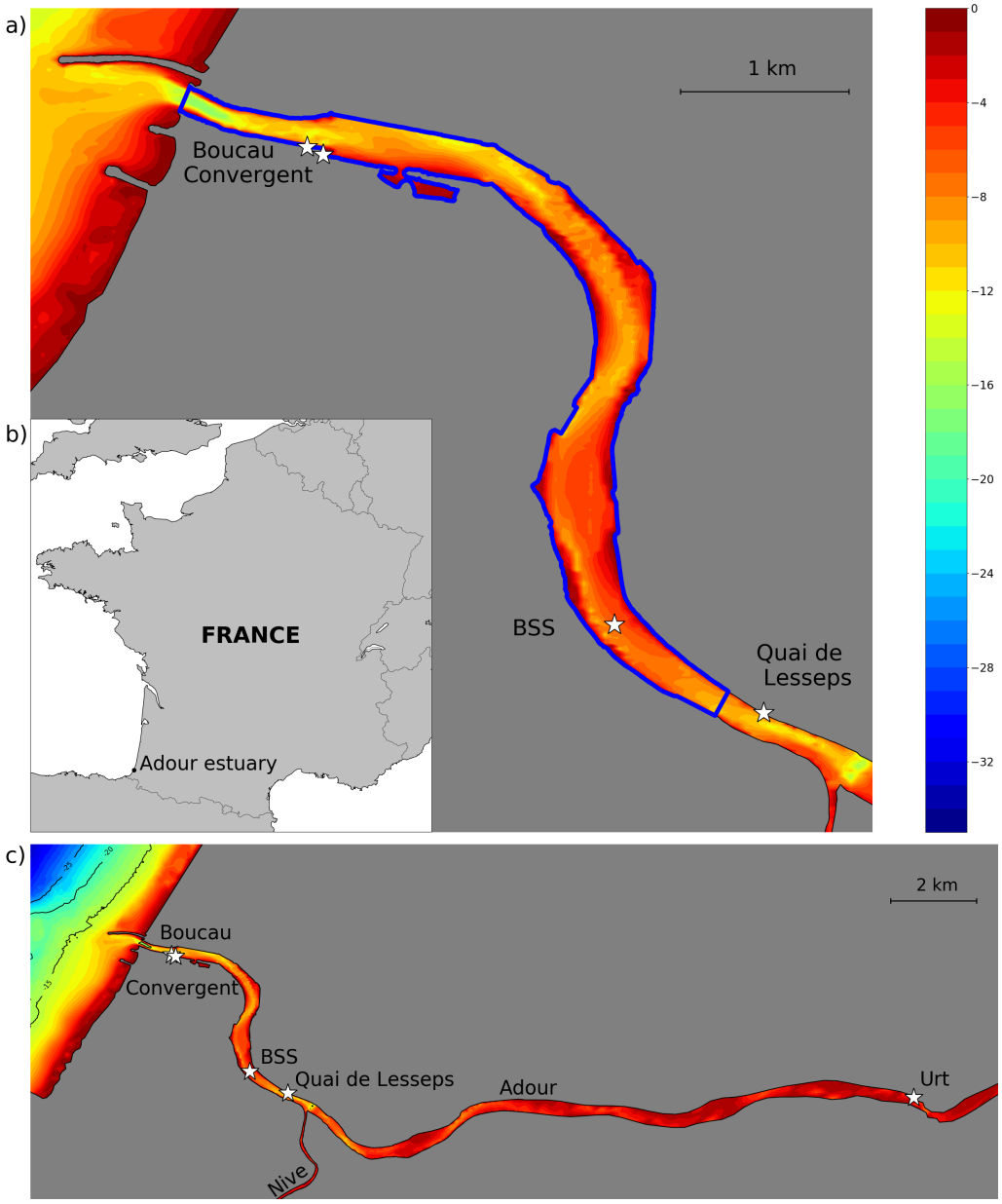

Figure 1: a) The study area, i.e. the last 6km of the estuary , with the Bayonne Harbor in blue. b) The location of the Adour estuary along the French coast. c) The Adour estuary from the entrance to Urt village. BSS white star is the boat survey station location. Boucau, Convergent, Quai de Lesseps and Urt white stars are the tide gauges locations. Colors represent the bathymetry in meter below the chart datum.

2.2. Field experiments

The objective of the present field experiments is to study the tidally-driven hydrodynamics inside the lower estuary, including salt-wedge, stratification, mixing and SPM dynamics. The field campaigns are based on a series of operations aiming to investigate the effect of river discharge and tidal range on the estuarine dynamics. For the sake of simplicity, the experimental results will be organized and named following the forcing conditions: LD/HD will refer to low/high river discharge and ST/NT will refer to spring/neap tide conditions, respectively, while the year is added at the

end. For instance, LD-ST17 will refer to data recover in low discharge and spring tide conditions in 2017. A summary of conditions during the boat survey measurements is given in Table 1, while each type of measurement is described herebelow. The measurements have been undertaken only in the last 6km of the estuary, in between the mouth and the confluence with the Nive river (Fig. 1 b)).

	Conditions		
	Date	T.R. (m)	Disch. (m^3/s)
LD-ST17	Sept, 19-20 2017	3.2-3.8	84-86
LD-NT17	Sept, 28-29 2017	1.2-1.3	112-128
LD-ST18	Sept, 25 2018	3.3	103
HD-ST18	June, 12 2018	3.2	1421

Table 1: Experimental conditions. LD/HD refer to low/high discharge conditions, respectively. ST/NT refer to spring/neap tide, respectively. T.R. and Disch. are the tidal range and river discharge, respectively.

2.2.1. Bottom moored measurements

A bottom-moored station has been deployed, at about 5 km from the entrance of the estuary, at the same location than the boat survey station (BSS on Fig. 1), in September 2017. Velocity profiles were recorded by a Flowquest ADCP (600 kHz) every 15 min (time averaged 5-min burst data at 4Hz), with a vertical resolution of 0.5m. The ADCP was located at 0.56 m above the bed. Velocity profiles recorded during LD-NT17 are presented in figure 4.

2.2.2. Fixed boat surveys

The fixed boat surveys were dedicated to the vertical structure of velocity, salinity, temperature and turbidity. Measurements were performed from an anchored boat (BSS on Fig. 1).

The salinity, temperature and turbidity measurements were carried out by a Seabird C19plus CTD sensor or a YSI 6920 probe. For each experiment, five-litre water samples have been taken to calibrate the instruments. Forty kilograms weights were attached to the measurements line in order to ensure the verticality. Probes measurements were recorded at 4Hz for the Seabird C19plus and 1Hz for the YSI 6920. Temperature data will not be discussed in this paper, due to negligible contributions in the density variations compared to salinity effect.

In addition to water properties measurements (1 profile every 15 min), high-frequency velocity profiles were recorded, for LD-ST18 and HD-ST18 only, by a Nortek Signature 1000 current profiler (ADCP) secured along the hull. The ADCP was continuously sampling at a rate of 8Hz with 20 to 30 cm cells.

2.2.3. Longitudinal sections

Longitudinal transects were realised across the control area (from 1 km to 5.5 km, from the entrance of the estuary) with an OSIL Minibat under-water towed vehicle, equipped with a multi-parameter probe. Salinity, temperature, pressure and turbidity have been recorded by the Minibat. Deployments have been carried out during LD-ST17 and LD-NT17 experiments (see Fig. 3 and 5, respectively). While the Minibat provides useful spatial information, its deployment remains a very delicate operation in such a shallow and vertically sheared navigation channel. The transects

were surveyed following the centre axis of the estuary, i.e. not always in the main channel due to navigation constraints near the docks.

2.2.4. Water levels

The tide gauge data presented hereafter have been collected either by Convergent or Bayonne-Boucau tide gauges, due to episodic malfunctioning. Both are operated by the Service Hydrographique et Océanographique de la Marine (SHOM) and located near to the entrance of the estuary (Fig. 1). In this paper, those data will be presented in water elevation above the local chart datum (in m C.D.).

2.3. Data processing

2.3.1. Velocity measurements

For each profiler, the velocity data are projected into a local coordinate system with the x axis directed along the channel with positive values landward, the y axis directed laterally towards the right bank, and the z axis directed upward. For simplicity, the generic term "velocity" generally refers later on to the x-component of velocity, otherwise clarification will be given.

High frequency velocity data from LD-ST18 and HD-ST18 are used to analyse turbulence properties. The 8Hz, 1s averaged, ADCP data of opposing beams (b_i) have been split into a mean ($\overline{b_i}$) and a fluctuating part (b_i'), using a sampling interval of 10 min. An additional high-pass filter is applied to remove low frequency fluctuations due to ship motion. The along-beam velocities have been used to estimate the components of Reynolds stress [34, 60, 46], as follows :

$$-\overline{u'w'} = \frac{\overline{b_3'^2} - \overline{b_1'^2}}{4sin(\theta)cos(\theta)} \tag{1}$$

$$-\overline{v'w'} = \frac{\overline{b_2'^2} - \overline{b_4'^2}}{4sin(\theta)cos(\theta)} \tag{2}$$

where θ represent the angle of each beam from the axis of the instrument ($\theta = 25^o$ for Nortek Signature 1000 ADCP).

The eddy viscosity is classically computed following the flux-gradient hypothesis:

$$\nu_t = -\frac{\overline{u'w'}}{\partial\overline{u}/\partial z} \tag{3}$$

The rate of Turbulent Kinetic Energy (TKE) production is expressed as a product of stress and shear :

$$P = -\rho\overline{u'w'}\frac{\partial\overline{u}}{\partial z} - \rho\overline{v'w'}\frac{\partial\overline{v}}{\partial z} \tag{4}$$

2.3.2. Richardson number

The non-dimensional Richardson number Ri is often used to quantify the stability of the density stratification in sheared flow [53]. A threshold value of 0.25 is commonly applied to distinguish stable stratification from unstable situation due to the breakdown of stratification by turbulent mixing. For high values of Ri, the buoyancy forces driven by the vertical density gradient are expected to

overcome and suppress turbulent mixing. The Richardson number formulation is here calculated from the ratio between density and mean velocity gradients:

$$Ri = -\frac{g}{\rho_0}\frac{\partial\rho/\partial z}{(\partial\overline{u}/\partial z)^2} \tag{5}$$

where ρ_0 is the depth-averaged density. For the calculation of the Richardson number, density is estimated according to UNESCO formula and density profiles are interpolated over the ADCP regular measurement positions. It should be noted that in figure 2, the top of the water column is missing in some salinity and SSC profiles due to the malfunctioning of our multi-parameters probe.

2.3.3. Turbidity and SSC

Turbidity profiles from boat surveys during LD-NT17, LD-ST18 and HD-ST18 have been converted into suspended sediment concentration (SSC) using a series of five-litre water samples and pre-weighted glass fiber filters.

3. Results

The presentation of the field results will first focus on salinity structure and circulation, based on the time evolution of the vertical profiles of the measured parameters (Figs. 2, 4 and 6 for LD-ST18, LD-NT17 and HD-ST18 cases, respectively) together with longitudinal sections (Figs. 3 and 5 for LD-ST17 and LD-NT17 cases, respectively). The LD-ST18 and HD-ST18 data are also depicted as temporal contour plots in Figures 7 and 8, respectively. For theses cases, additional turbulence data over the whole water column, including estimates of eddy viscosity and rate of TKE production, are then presented from hull-mounted ADCP measurements, to analyse the competition between turbulence and stratification. SPM dynamics is finally explored in the view of previous observations on estuarine dynamics.

3.1. Estuarine salinity structure and circulation

Figures 2, 4, and 6 present the tidal evolution of velocity, salinity and Suspended Sediment Concentration (SSC) profiles, during the dry season, for spring (LD-ST18) and neap (LD-NT17) tide conditions, and during the wet season for spring tide (HD-ST18) respectively. Figures 3 and 5 display vertical salinity and turbidity structure along the last 6 km of the estuary, from Minibat measurement during LD-ST17 and LD-NT17 experiments, respectively.

The data analysis is first focused on the spring tide condition during the dry season (Fig. 2 and 3). The ebbing tide is characterised by a horizontal salinity gradient (Fig. 2 (c) and Fig. 3 (b)), with a homogeneous water column flowing out the estuary. As the ebb progresses, the water column becomes fresher and flows faster. At low water (11:36), the seaward current shows a strongly sheared structure, with a nearly linear profile across the water column. Progressively, the water column slows down and the salinity still decreases homogeneously along the water column. As the tide rises, the salinity at the top of the water column goes on decreasing, while, at the bottom of the water column the salinity increases. Salinity profiles are not homogeneous anymore, and the salinity gradient increases. The current reversal occurred around 13:30 (i.e. almost 2 h lagged from the low water time). The velocity profile reveals a typical salt-wedge profile, when the salty marine waters flow into the estuary. A fast landward salty bottom layer is observed in the lower 3m, while

an oppositely fresh upper layer is still flowing seaward with a sheared profile. The salinity reaches its minimal value in the surface layer, when the salt-wedge starts entering the estuary. The salty bottom layer, which is rather well-mixed, increases both in thickness and salinity as the tide rises. At the end of the flood tide, the full water column is salty and flows upstream, blocking the fresh water inside the upper part of the estuary. The continental waters blocked into the upper part of the estuary during the flood, are then released during the ebb. This mechanism, named "pulsed plume mechanism", has already been highlighted by Dailloux [8].

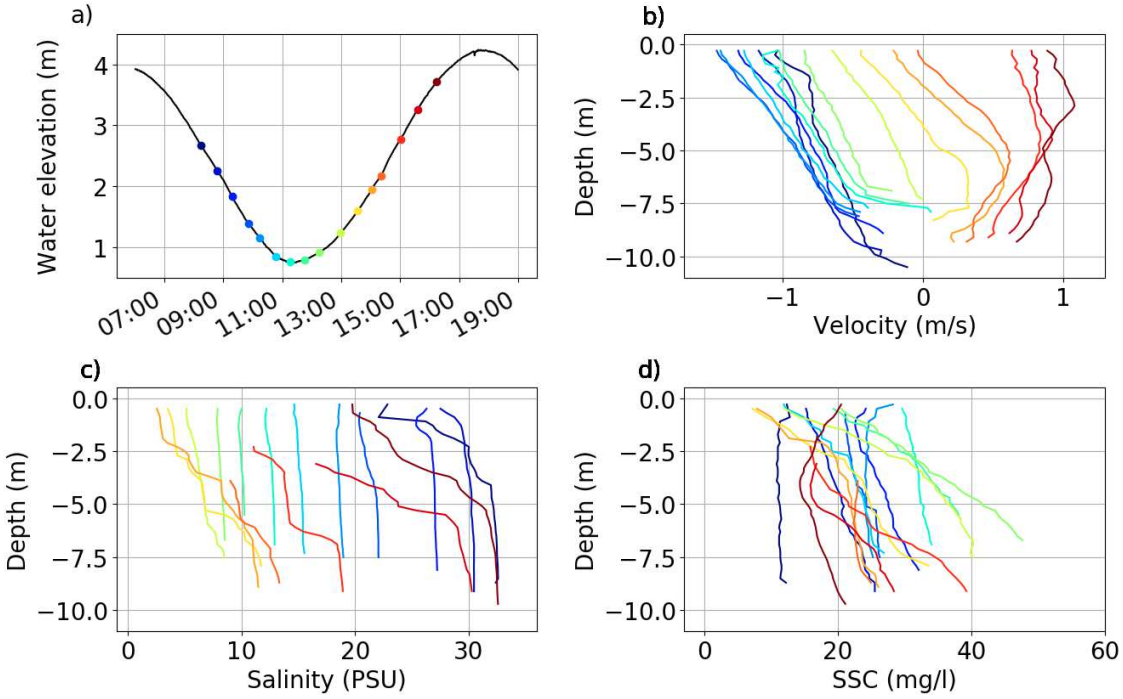

Figure 2: Tidal dynamics from LD-ST18 fixed boat surveys during low discharge spring tide conditions. (a) Water level and timing of measurements. (b), (c), and (d): velocity, salinity and SSC profiles. Note that the same data is presented in contour plots in Figure 7.

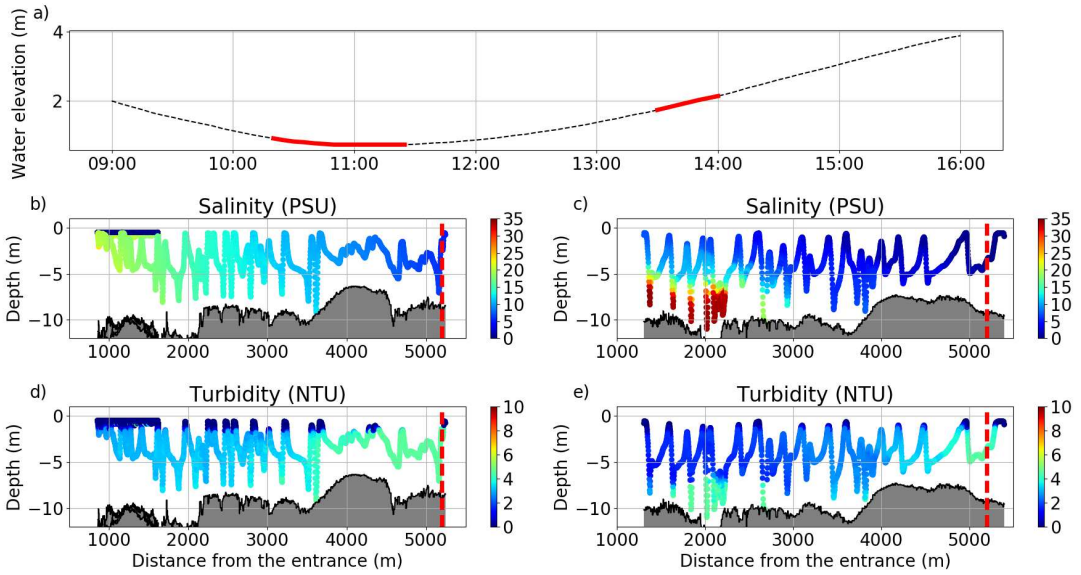

Figure 3: Longitudinal and vertical structure across the lower estuary from Minibat measurement during LD-ST17 experiment. (a): Water elevation with measurement periods highlighted in red. (b) and (c): salinity data for falling and rising tide. (d) and (e): turbidity data for falling and rising tide. The bed of the estuary is represented in grey. The red dashed line represents the BSS location.

The contrast between spring tide and neap tide (Fig. 4 and 5) is straightforward, as during neap tide the salinity stratification is maintained all along the tidal cycle and the velocity magnitudes are reduced. At the end of the flood (11:00), a sharp pycnocline separates a two-layer flow, with denser marine water flowing upstream underneath fresh continental waters. The bottom saline layer grows thicker until post-high tide slack water (14:00). Unlike spring tide, at neap tide the pycnocline is not able to reach the surface. The current reversal is lagged of almost 3h from the high water (10:49). As flow reverses seaward, the pycnocline thickens and deepens, while the surface and the bottom salinity remain relatively constant. This time the ebbing shear velocity profiles are associated with a vertical stratification. This permanent stratification leading to an inhibition of the salt-wedge flushing during neap tide is generally associated with stagnant waters and hypoxia [29, 3].

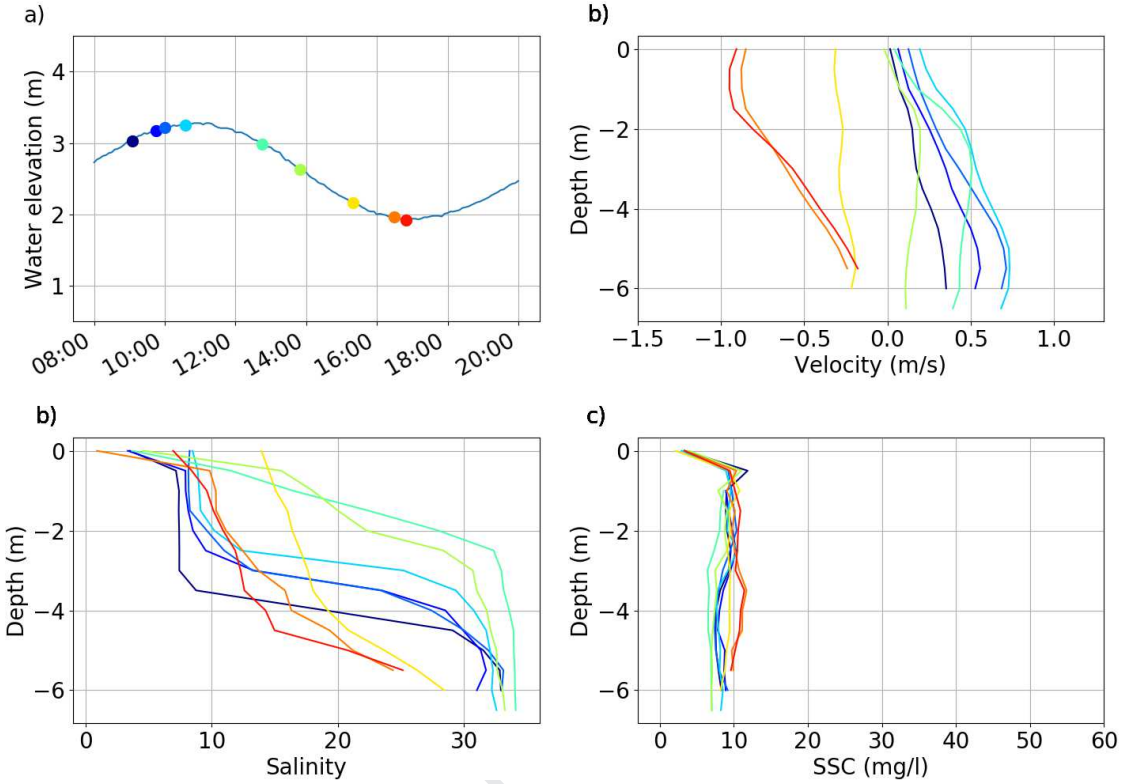

Figure 4: Tidal dynamics from LD-NT17 fixed boat surveys during low discharge neap tide conditions. (a) Water level and timing of measurements. (b), (c), and (d): velocity, salinity and SSC profiles.

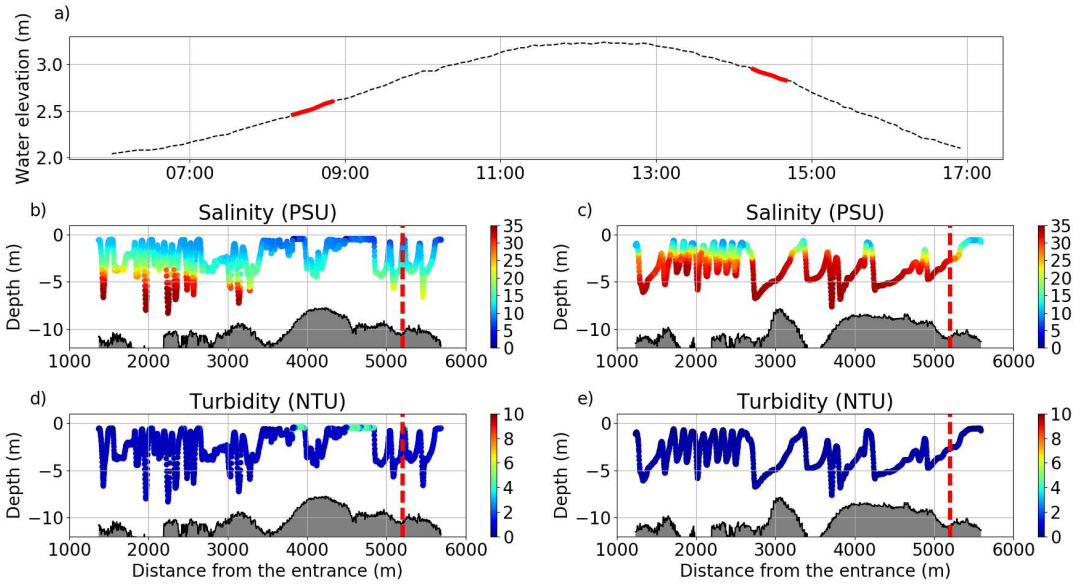

Figure 5: Longitudinal and vertical structure across the lower estuary from Minibat measurement during LD-NT17 experiment. (a): Water elevation with measurement periods highlighted in red. (b) and (c): salinity data for falling and rising tide. (d) and (e): turbidity data for falling and rising tide. The bed of the estuary is represented in grey. The red dashed line represents the BSS location.

A dedicated experiment (HD-ST18) was carried out during a high discharge event in order to explore the role of river runoff on the hydro and sediment dynamics compared to the reference low river discharge dataset presented hereabove. Figure 6 depicts the time evolution of velocity profiles, salinity and Suspended Sediment Concentration (SSC) profiles during high river discharge conditions. The comparison with low discharge conditions presented in Figure 2 shows the drastic influence of river run-off on the estuarine dynamics. Similar maximal magnitudes are reached during the ebb, but the velocity profile is almost constant, and the water column is homogeneously fresh. As tide rises, the water column shows a piston-like behaviour, i.e. marine water impounding river water into the estuary with a quasi uniform velocity along the vertical. The current reversal (13:00) occurs much later for the high discharge case, i.e. almost three hours after the low water (09:58), than for the low discharge case. The piston-like behaviour remains active all along the flow reversal and during the most part of the flood tide. This greatly differs from the low discharge case for which a vertical shear of velocity is systematic at the early stage of flood tide. At the very end of the flood (16:00), the salt-wedge is finally able to reach the measurement area. A 2 m thick bottom salty layer propagates upstream at about 0.5 m/s. The high river discharge is again responsible for a significant time lag compared to low discharge conditions for which the salt-wedge was able to reach boat survey station about 2 h earlier. A remarkable observation, at the salt-wedge arrival, is the rapid seaward reversal of the overlying fresh water layer. The water column forms, therefore, a two-layer vertical structure with strong vertical shear in velocity and a sharp pycnocline. Note that the seaward/landward velocity maxima are reached in the upper parts of the pycnocline and of the salt-wedge, respectively.

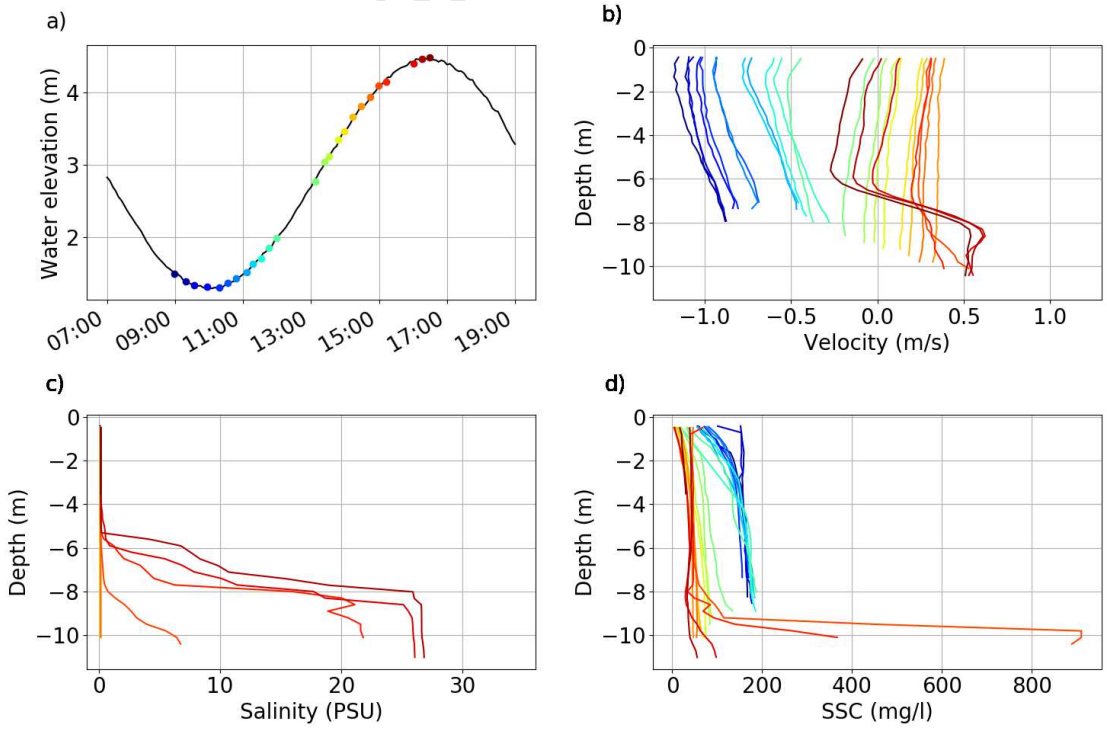

Figure 6: Tidal dynamics from HD-ST18 fixed boat surveys during high discharge spring tide conditions. (a) Water level and timing of measurements. (b), (c), and (d): velocity, salinity and SSC profiles. Note that the same data is presented in contour plots in Figure 8.

3.2. Turbulence properties

The previous section revealed the complex vertical salinity structure and circulation taking place into the Adour estuary. This first result needs to be further investigated by a turbulent properties analysis, to get a better understanding of the interaction between stratification and turbulent mixing. The representation of Richardson number profile as $log_{10}(Ri/0.25)$ is used in figures 7 and 8 to easily estimate the stability of the water column: stable (unstable) flows are expected for positive (negative) values. In addition, high-resolution high-frequency velocity profiles are used to infer turbulent properties of the flow. Figures 7 and 8 shows the tidal evolution of the vertical distribution of turbulent properties at the survey station BSS for the low (LD-ST18) and high (HD-ST18) river discharge experiments respectively.

Figure 7 depicts the data recovered during spring tide and low discharge conditions (LD-ST18). At 08:15, the water column is slightly stratified and the production of turbulence is focused in a very thin layer above the bed related with weak turbulent diffusion in most of the water column. As the water column becomes homogeneous and ebb current accelerates during the estuary flushing, the turbulence spreads into the water column aside from in the 2 m surface layer. The turbulent mixing overcomes the buoyancy forces and water column becomes fully unstable ($log_{10}(Ri/0.25) < 0$). Maximal values of P_{tke} and ν_t are associated with maximum ebb currents. The eddy viscosity is maximal in the bottom 4 m and reaches typical values (about 1.5 10^{-2} $m^2.s^{-1}$) measured in estuary for similar velocity and stratification conditions [46]. Those measurements also confirms that the eddy viscosity decreases toward the surface [35]. The slack water and the subsequent flow reversal are associated with a drastic drop of turbulence production. After 13:00, the sign change of the Richardson number indicates the shift toward a stable stratified situation which further reduces the eddy viscosity. At the salt-wedge entrance (around 13:30), a stable stratification develops with no turbulent mixing except an increase of TKE production and eddy viscosity at the tip of the salt-wedge. High values of Richardson number are associated to the edges of the pycnocline. Burst of turbulent production seems to develop in the upper layer between 14:00 and 14:30, which may correspond to a local destabilisation of the sheared layer. As the tide rises, the water column turns on stable up to the surface with no more turbulent mixing.

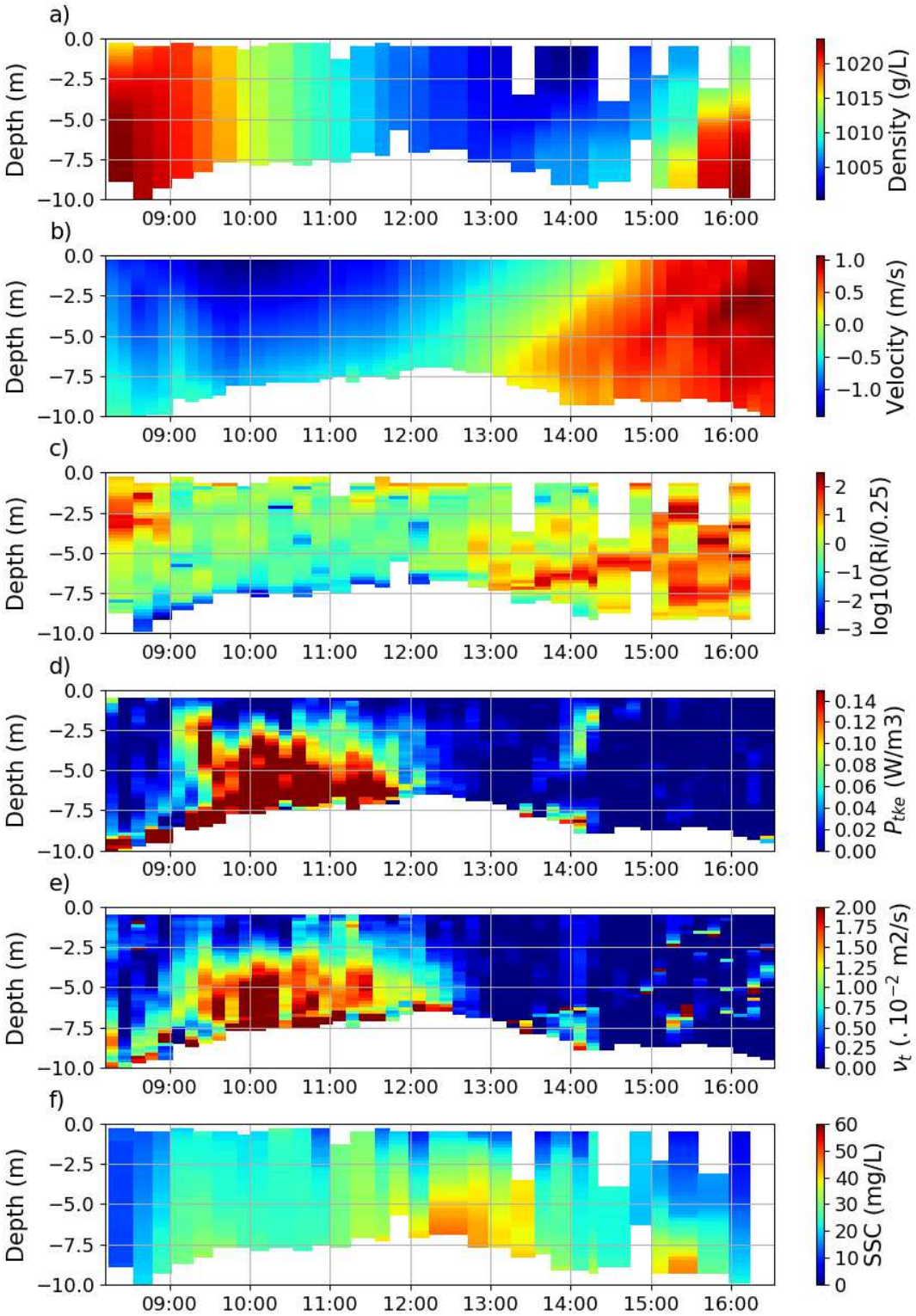

Figure 7: Tidal evolution during LD-ST18 experiment : (a) vertical structure of density, (b) time-averaged velocity, (c) Richardson number, (d) production rate of TKE, (e) eddy viscosity, and (f) suspended sediment concentration.

In addition, Ri calculations (not shown here) have been carried out for neap tide conditions based on profiles shown in figure 4. As expected, the nearly permanent vertical salinity stratification promotes stability throughout the water column.

Figure 8 presents similar data than figure 7, but applied on data collected under high river run-off conditions. It is first recalled that Richardson number should be considered with respect to the corresponding velocity and density profiles: nearly neutrally stratified conditions (i.e. unstable conditions) may appear stable in terms of Richardson number when the velocity shear is very weak. This is for instance the case in the surface layer (Fig. 8). During high discharge conditions, the lower estuary is filled with fresh water for most of the tidal cycle, the only exception being the salt-wedge arrival just before high tide (15:00). Therefore, the turbulent properties variations drastically differ from the low discharge case shown in figure 7. At the end of the ebb tide (before 10:00), the water column is fully fresh and has an almost constant velocity. High rate of TKE production and eddy viscosity are measured at the peak of ebb currents. The strong discharge is able to maintain the instability and a significant TKE production until 12:00 (i.e. more than two hours after low tide). Then, slack water (around 13:00) is associated to a strong drop of turbulence production and eddy viscosity, which remains very weak until the arrival of the salt-wedge. However, the piston effect is clearly visible at rising, with nearly vertically uniform velocity profiles during most of the rising tide. The consequence, in term of stability, is that the lower estuary remains unstable all the time until the salt-wedge is able to reach the measurement station (15:00). A first moderate rise of TKE production is observed near the bottom to a depth of 3m, which indicates that the tip of the salt-wedge is a mixing zone. From that moment, one notes the development of a 1 to 2 m high pycnocline, both strongly stratified and very sheared. Corresponding positive values of Richardson number indicates the stability of the sheared layer. Peaks of Richardson number are observed near the edges of the pycnocline, associated to more stable areas, whereas the core of the sheared zone is very close to the instability threshold. The TKE production strongly rises near the bottom, but remains confined near the bottom layer by the effect of overlying stratification. It can be noticed that, even if the velocity of entering marine waters is much lower than for the low discharge case, a much stronger turbulent mixing is observed in the bottom layer. The salt-wedge arrival (15:00) is a striking example of a dynamical competition between turbulent mixing and stratification: turbulent diffusion is very active near the bottom and below the pycnocline, but totally vanishes in the overlying fresh water layer.

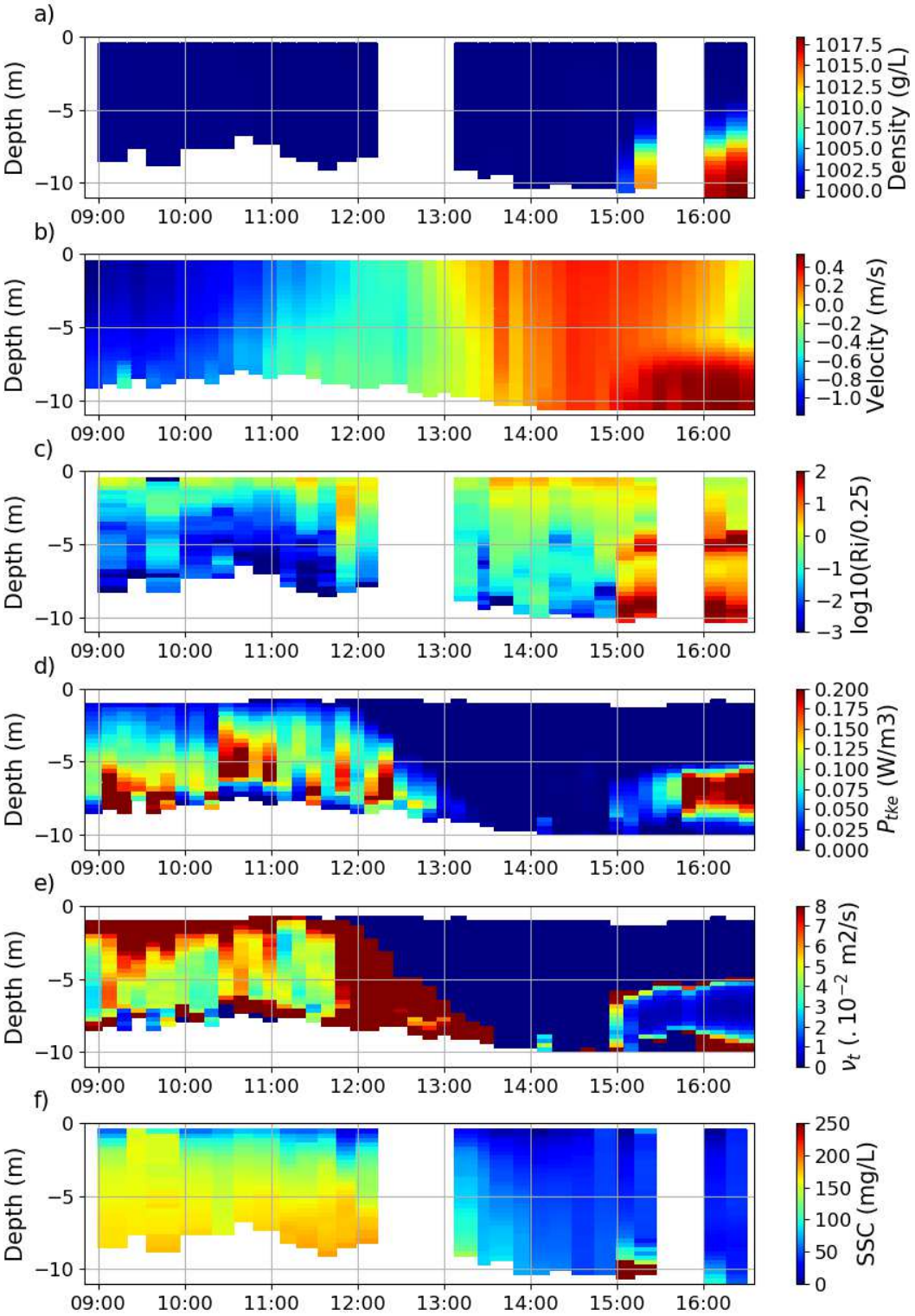

Figure 8: Tidal evolution during HD-ST18 experiment : (a) vertical structure of density, (b) time-averaged velocity, (c) Richardson number, (d) rate of TKE production, (e) eddy viscosity and (f) suspended sediment concentration. Note the difference in range compared to Figure 7.

3.3. Suspended sediment dynamics

This section is dedicated to the response of the sediment load to the complex hydrodynamics of the lower Adour estuary presented above. Figures 2 (d), 4 (d) and 6 (d) represent the SSC profiles collected during LD-ST18, LD-NT17 and HD-ST18 respectively. Figures 7 (f) and 8 (f) display same data as presented in Figures 2 (d) and 6 (d) under timeseries color plots. Figures 3 (d), (e) and 5 (d), (e) show Minibat turbidity data collected during LD-ST17 and LD-NT17 respectively.

First, a focus on the low river discharge reference case allow us to study the effect of tidal cycle on sediment dynamics, such as erosion, advection and deposition mechanisms. In Figures 2 and 7, it can be noticed that at mid-ebb, the full water column is flowing out the estuary and the vertical velocity gradient is increasing. It results in a sufficient bottom shear stress to re-suspend sediment around 08:30. The sediments are maintained in suspension and are able to reach the surface of the water column by the turbulent mixing appearing at 09:00. Figure 3 shows that a horizontal gradient of SSC associated to the horizontal gradient of salinity develops, with SSC increasing as the water becomes fresher. These sediments in suspension are advected seaward by the flow, at a velocity that can reach 1.5 $m.s^{-1}$ in the surface. Approaching the slack water period (12:00), the ebbing velocity is less than 0.6 m/s (green profiles on Fig. 7) and the vertical gradient of velocity decreases. Consequently the re-suspension capacity of the flow decreases. The turbulence maintaining the sediment in suspension also drops down, and so the SSC develops a vertical gradient, which might be associated to settling. It progressively leads to an overall SSC decrease. Around 14:00, sediments accumulated at the bottom of the water column are advected landward by the entrance of the marine waters into the estuary, while sediments located at the surface are still advected seaward. At 15:00, an area of high turbidity is generated at the tip of the salt-wedge front. This trend is generally attributed to the accumulation of sediments due to the convergence of sediment fluxes from the river and the ocean. This peak of SSC is contained near the bottom by the pycnocline. Another striking feature is the decrease of SSC in the layer of fresh continental water flowing above the salt-wedge (Fig. 7 and 3). This observation should likely be attributed to the stratification-induced damping of turbulence, leading to particles sinking, as previously observed in other systems [59, 18]. At 16:00, velocity profiles are much more homogeneous and the turbulence is damped by the stability of the two-layer flow, and so the SSC decreases.

The tidal range has also a striking effect on the above mentioned sediment dynamics, as shown by the comparison between Figures 2 and 4. During neap tides, the SSC remains very low, about 10 $mg.L^{-1}$ all over the tidal cycle and quite homogeneous over the water column, while during spring tides, the SSC is generally stronger (up to 45 $mg.L^{-1}$) and slightly more variable throughout the tidal cycle. This very low SSC can be explained by a permanent stratification and a reduced velocity. Low velocities impede the re-suspension of sediments and the permanent stratification damps down the turbulence. The sediments can therefore not remain in suspension. During neap tides the flushing capacity is drastically reduced by the absence of re-suspension and advection and the strong deposition.

The riverine forcing also influences the sediment dynamics, as highlighted by Figures 6 and 8. During high river discharge, the ebbing currents are reinforced and the flow is much more turbulent, resulting in a stronger re-suspension and seaward advection. Consequently, SSC values are much more higher than those observed during low discharge conditions. In Figure 8, it can be noticed that during the ebb, the SSC is quite homogeneous in the water column, with values about 150

$mg.L^{-1}$. These reinforced re-suspension and advection result in a very good flushing capacity of the estuary. At 11:30, both flow and turbulent mixing reduce in intensity. The particles are not anymore maintained in suspension and a progressive sedimentation can be observed. The SSC shows a pattern similar to the one of turbulent properties. Between 15:00 and 17:00, the piston-like behaviour occurs pushing slowly the full low SSC water column landward. Similarly to the low discharge conditions, the salt-wedge passing (15:00) corresponds to the higher measured SSC. However, during high river discharge, the SSC is able to reach up to 850 $mg.L^{-1}$ in the bottom layer. The increased river flow reinforces the convergence mechanism. These sediment in suspension are also contained by the pycnocline and advected landward, while the surface waters containing little sediments are advected seaward. Around one hour after the salt-wedge front passing, the SSC at the bottom of the water column has decreased to about 100 $mg.L^{-1}$. This high turbidity area is thus supposed to follow the up estuary motion of the salt-wedge leading front.

4. Discussion

This article presents a set of field observations carried out to improve the knowledge about circulation and sediment transport into the lower Adour estuary. These results provide the first in-situ characterisation of the hydrological functioning of the Adour lower estuary, but also give rise to a number of questions. Discussion points have been organised under three main topics: estuarine salinity structure and circulation, sediment dynamics and connection to plume dynamics.

4.1. Estuarine circulation

The present *in-situ* dataset revealed the high variability of the Adour lower estuary, in terms of hydrological functioning. A salt-wedge generally develops during the flood tide in the Adour lower estuary. This salt-wedge depends on river discharge, by being more steeply marked during the wet season due to intense river forcing. In addition, the tidal forcing is also an important driver of the Adour estuary (mesotidal system) with a significant effect of the spring/neap cycles on the estuarine salinity structure. Under low discharge conditions, the neap tides are associated to fully vertically stratified estuary along the tidal cycle, while during spring tide the salt-wedge shape is lost during the ebb, and an horizontal salinity gradient takes place. Such a versatility in the salinity circulation in response to the fluctuations of tidal and fluvial forcing can not be properly accounted for by usual descriptive estuary classifications, such as, e.g. the well-know scheme of Cameron and Pritchard [7]. More physical insight is provided by the recent quantitative scheme of classification developed by Geyer and MacCready [21].

The scheme of classification developed by Geyer and MacCready [21] investigates the respective contribution of tidal mixing and stratification by the means of a two parameters space : the freshwater Froude number $Fr_f = U_R/(\beta g s_{ocean} H)^{1/2}$ and the mixing parameter $M = \sqrt{(C_D U_T^2)/(\omega N_0 H^2)}$, where U_R is the net velocity due to river flow (i.e. the river volume flux divided by the estuarine section), β is the coefficient of saline contraction, g is the acceleration due to gravity, s_{ocean} is the ocean salinity, H is the water depth, C_D is the bottom drag coefficient, U_T is the amplitude of the tidal velocity, ω is the tidal frequency and $N_0 = (\beta g s_{ocean}/H)^{1/2}$ is the buoyancy frequency for maximum top-to-bottom salinity variation in an estuary. The former dimensionless parameter Fr_f compares the net velocity due to river flow and the maximum possible front propagation speed, while the latter M assesses the role of tidal mixing and the influence of stratification on the vertical

mixing. Due to spring/neap variations and wet/dry seasons changes, estuaries are not represented by a point in this classification scheme, but rather by rectangles covering the range of observed regimes. An adaptation of the Geyer and MacCready's regime diagram [21] is proposed in Figure 9, with the M and Fr_f ranges reached by some well-documented estuarine systems in order to easily compare with the Adour estuary.

Of particular interest is to know the extent to which the variability of the Adour estuary can be described by such approach and to evaluate how it can compare to other typical systems selected for their contrasted dynamics. For the calculation of both parameters, we considered $\beta = 7.710^{-4} PSU^{-1}$, H to be a characteristic value of the water depth $H = 10m$, the salinity of ocean $s_{ocean} = 34.5$ PSU. A first remark should be made on the uncertainty on the estimation of the mixing parameter M. This parameter shows a strong sensitivity to both U_T and C_D values, which are not straightforward to estimate. In Geyer et al 2014 [21], U_T is defined as the amplitude of the depth-averaged tidal velocity, while it has been estimated as the rms velocity 3m above the bed in Geyer et al 2000 [20] and considered equivalent to the maximal velocity in Li et al 2014 [33]. For the present study, the reference value of U_T is provided by rms depth-averaged velocity measured at the BSS bottom moored station (Fig. 1). The bottom drag coefficient C_D can also be strongly spatially variable inside an estuary, and relatively challenging to estimate. In Geyer et al. 2014 [21] authors consider that C_D generally varies between 1 to 2.5 10^{-3} inside an estuary, while Geyer et al. 2010 [17] mentioned a value of C_D generally about 3 10^{-3} inside estuaries. For the Adour estuary, two point currentmeters deployed in the bottom layer have been used by Sous et al [47] to estimate a C_D value about 1.5 10^{-3} between Convergent and BSS stations, which is used here as a reference for the estimation of M. Using data collected inside the Adour estuary, U_R estimation ranges from 0.05 to 0.75 $m.s^{-1}$, therefore Fr_f should range from 0.03 to 0.46 for low to high discharge conditions,respectively. The mixing parameter M, based on reference values for U_T and C_D, ranges from 0.36 to 0.66 for neap to spring tide conditions, respectively (Fig. 9, solid line rectangle). In order to illustrate the M sensitivity to U_R and C_D parameters, estimating now U_T as the maximal entering velocity together with a C_D value of 3 10^{-3} will shift the Adour's system toward higher ranges of mixing parameter values (0.68 to 1.13), see dashed line rectangle in Figure 9. In addition, the values of the mixing parameter might be further increased with data from neap tide conditions combined to high river run-off, which are not documented by the present dataset.

Keeping in mind these limitations, the estuarine parameter space diagram proposed by Geyer and MacCready [21] confirms the variability of the hydrological functioning of the Adour estuary in comparison with other typical systems (Fig. 9). Noted that the large area covered by the Adour river in this diagram is due to the highly contrasted hydrological conditions encountered during our measurements. Others systems may have been observed only during mean hydrological conditions, leading to reduced rectangles. Based on collected data, presented in this paper, we can analyse the observed dynamics of the Adour estuary. Under high tidal mixing conditions (i.e. high M value), the Adour river dynamics is quite similar to those of Fraser [19], Changjiang [33] and Merrimack rivers [41], which are all considered as time-dependent salt-wedge estuaries. Those energetic and stratified estuaries are characterised by strong tidal and fluvial velocities (Fig. 10). It results in a strengthened stratification during the flood, that weakens during the ebb tide, where the turbulence develops in the full water column. Under low tidal mixing conditions (i.e. low M value), the Adour tends to show a behaviour similar to the Ebro river. This latter has a

similar shape and river discharge than the Adour, but the microtidal regime (associated to a small M) results in a stagnant salt-wedge under low river run-off ejected out of the estuary when the river discharge exceeds 500 $m^3.s^{-1}$ [25]. Measurements undertaken during neap tide and low river discharge in the Adour estuary reveal a similar pattern with an almost stagnant salt-wedge and strong stratification. Unfortunately, observations were not carried out during neap tide and high river discharge (around 1500 $m^3.s^{-1}$), but we can expect an absence of the salt-wedge or at least a strong reduction of the saline intrusion. The role of river discharge is however clearly identified for spring tides, corresponding to fluctuations along the Fr_f axis in Figure 9 for large value of M. Under low river discharge conditions (i.e. low Fr_f value), the influence of tidal mixing is more important, leading to a smoother vertical stratification and a strongly stratified regime. During the ebb, the peak of turbulence can be sufficient to break down the vertical stratification and generate an horizontal stratification. This horizontal stratification is a typical attribute of partially mixed regime. When the river discharge increases (i.e. higher Fr_f values), the vertical stratification appears to be stronger, with a sharper pycnocline and a salt-wedge restricted in the lower part of the water column.

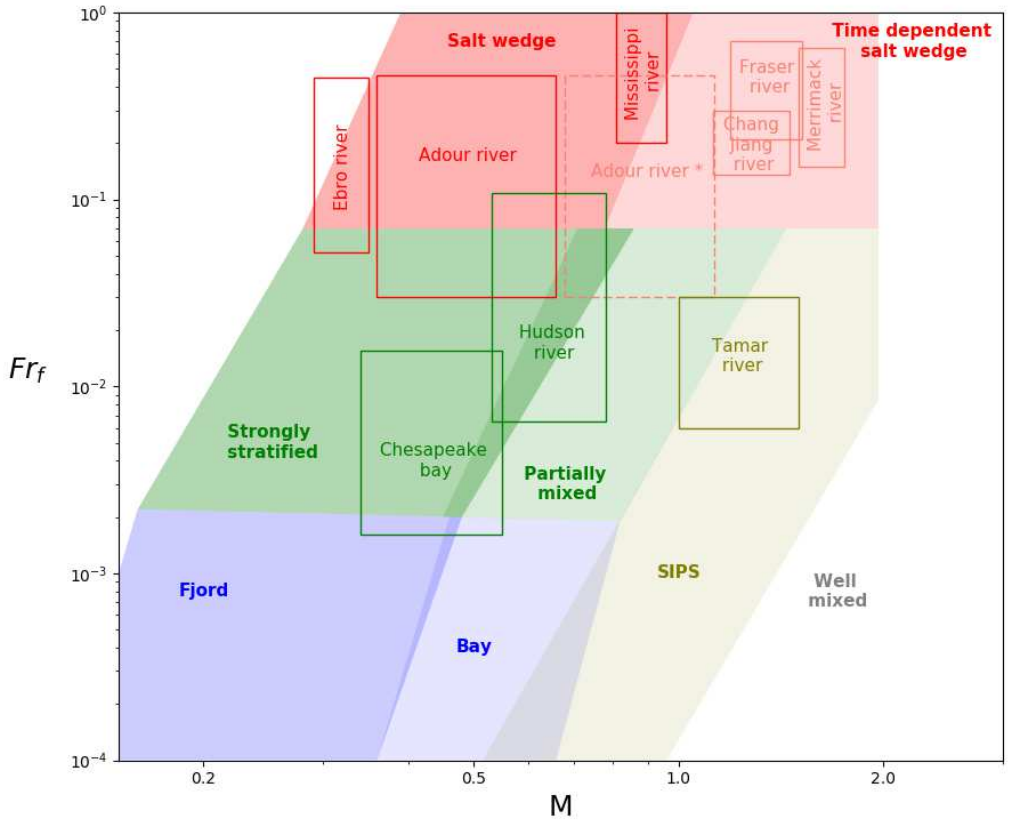

Figure 9: Estuarine classification based on the freshwater Froude number and mixing number, adapted from [21], Fig 6. (*) The dashed rectangle represent the location of the Adour river using other estimations of U_t and C_D.

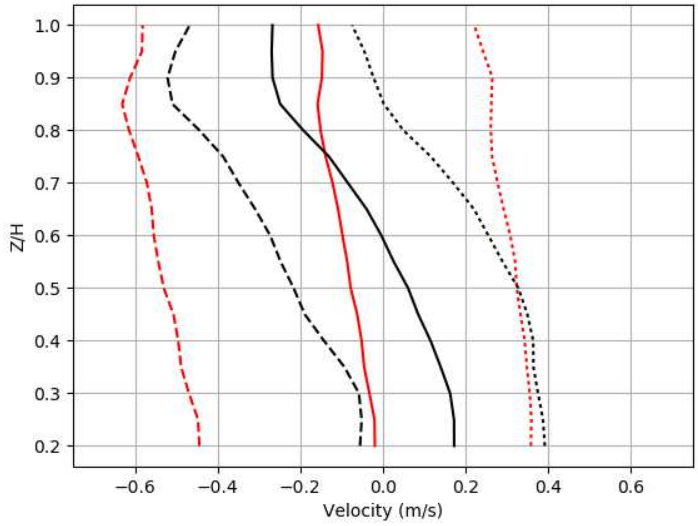

Figure 10: Tidally averaged velocity profiles for neap (full black line) and spring (full red line) tides with low river discharge. Flood (dotted lines) and ebb (dashed lines) average velocity profiles for neap/spring low river discharge conditions. Data from bottom moored station located at BSS location (Fig. 1)

The lateral dynamics, which has not been explored in the present data analysis, may play an additional important role in the estuarine circulation and salinity structure. Both local curvature of the lower estuary and cross-sectional bathymetric gradient are expected to favor a degree of three-dimensionality in the estuarine flow structure [31, 44]. This calls for further dedicated experimental campaign to better understand the contributions of along-channel and lateral components in mixing processes, and their dependencies on tidal range and river discharge.

4.2. Suspended sediment dynamics

The present study allows to analyse the impacts of physical processes taking place inside the Adour estuary on the observed sediment transport. Since the Glangeaud's pioneering description of an Estuarine Turbidity Maximum (ETM) in the Gironde estuary in 1938 [22], a series of numerical and experimental studies have revealed the importance of ETM in estuarine sediment dynamics [4, 27, 55, 6] among others. ETM have strong impacts on the marine and estuarine ecosystems, being a major driver of sediments, contaminants and nutrients from continent to ocean. ETM formation is primarily driven by the hydrodynamical functioning of the estuary. In salt-wedge systems, and in particular in the presence of strong tidal forcing, two key mechanisms have been identified in the ETM dynamics: the residual gravitational circulation and the tidal asymmetry. Burchard and Baumert [4] demonstrated that tidal asymmetry is of a bigger importance in the ETM formation than gravitational circulation in macrotidal salt-wedge estuaries. The gravitational circulation plays a part in sustaining and stabilising the ETM mass. In the Charente estuary, which shows similarities with the Adour in terms of dimension and salt-wedge regime but with a stronger tidal forcing, the tidal asymmetry is mostly responsible for the formation of the turbidity maximum, while the density gradient has an influence on its shape and its stratification [52]. More recently,

Olabarrieta et al. [36] have highlighted the role of density gradient-driven subtidal flows in the sediment import and trapping into the estuary associated to near-bed flood tide dominance.

Based on the present dataset, no stable ETM has been observed in the lower Adour estuary. Further insight is provided by analysing the main expected ETM drivers. First, the tidal assymetry in the Adour estuary has been studied based on the water elevations collected by tidal gauges along the estuary. Figure 11 outlines that a slight tidal asymmetry of less than 20 minutes exists in the lower estuary. Provided time lag appears too weak to generate an ETM when compared to the Charente estuary, where tidal asymetry can reach almost 3.8h at the river mouth [52, 51]. A strongest asymmetry can be noticed in the upper part of the estuary (i.e. 20 km upstream at Urt village). Such mechanism might generate on ETM in this reach of the estuary. Extended measurements until Urt village or a dedicated numerical study are foreseen as further work to estimate the impact of this tidal asymmetry on the sediment transport in the upper estuary. The second ETM driving process is the residual estuarine circulation. In most cases, no residual estuarine circulation has been observed in the lower estuary. The mean ebbing velocities are stronger than the mean flooding velocities, resulting in a good flushing of water masses and suspended sediment. The only exception is observed during very low river flow and tidal forcing conditions, as revealed by the residual tidally-averaged velocity profiles depicted in Figure 10, black solid line. In such conditions, a residual circulation is observed, but its effect in generating a well-developped ETM is likely compensated by limited resuspension due to reduced velocities. Note however that the bottom moored current profilers are not able to resolve the bottom 1.5 m (structure size and blanking zone), which can hide near-bed processes.

Moreover, it should be noted that riverine input of sediment is very low compared to other tidal estuaries, based on SSC obtained in the present conditions. Even during high river discharge, during the ebb, when the water column is full of fresh riverine waters flowing out the estuary, the SSC is about 150 $mg.L^{-1}$. This very low supply in sediment even during high river discharge might be related to the marshy meadows located along the Adour river, which could be responsible for particle trapping.

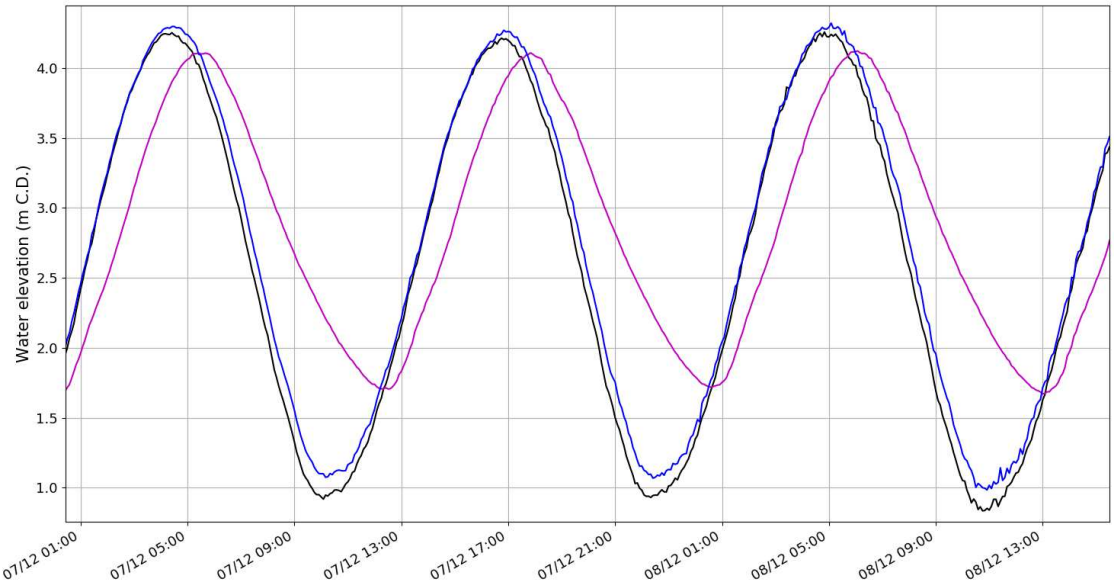

Figure 11: Water elevation data collected at Urt village (22 km from the estuary mouth, in magenta), at Convergent (700 m from the estuary mouth,in black) and Quai de Lesseps (5.6 km from the estuary mouth, in bleu) tide gauges, during spring tide.

The observed influence of tidal range on the lower estuary has also a strong effect on the ejected plume. At spring tide during the dry season, continental waters are blocked inside the estuary by the marine waters entrance for about three hours. This mechanism drives the pulsed behaviour of the plume of the Adour estuary already highlighted by Dailloux [8]. By contrast, at neap tide during low discharge conditions or under high discharge conditions, a layer of continental water is flowing seaward all along the tidal cycle at the top of the water column, almost constantly feeding the plume leaving the estuary with fresh water. The pulsed behaviour of the Adour estuary may take place only when the tidal forcing is able to overcome the riverine forcing, and so the riverine waters are blocked into the estuary by the marine water entrance.

4.3. Impacts of engineering works

The Adour estuary exhibits a strong variability of salinity, which has never been reported in the literature. This is highlighted by direct measurements in a range of conditions and confirmed by the Geyer and MacCready classification diagram [21]. Part of the observed variability is directly imposed by the fluctuations of the external forcing, i.e. a mesotidal regime associated with seasonal variations of river discharge driven by the oceanic climate and the close proximity to the Pyrenées mountains. However, such conditions may not entirely explain the observed variability of estuarine salinity circulation when comparing the Adour to other systems. It can be hypothesised that the artificial channelisation of the lower estuary coupling with strong dredging activities act to enhance the fluctuations in hydrological regimes. The Adour estuary is fully artificial since 1578, when the mouth of the estuary has been fixed in front of the Bayonne city by diking, under the decision of King Charles IX. In 1810, Napoleon decided to reduce the entrance of the estuary to 150 m in the aim of protecting the channel from sand accumulation by focusing the ebb energy. For a wider lower estuary, which would be likely the case in a more natural context, the U_R value would

consequently decrease and so the Fr_f. This reduction of river flow velocity should reduce the stratification within the estuary which should promote the development of strongly stratified or partially mixed regimes. These engineering works are complemented by dredging activities from 1896. Nowadays, the quantity of sediments to be dredged in the lower estuary per year is about 525000 m^3. The dredger of 1200 m^3 capacity operates almost everyday, except from June to September. This is also supposed to have a significant impact on the stratification, by maintaining the channel deeper. In the absence of dredging, the depth reduction would strengthen the river flow and decrease the tidal propagation speed, resulting in an enhanced mixing. Following the Geyer and MacCready classification [21], this would result in an increase of both parameters likely leading to a more systematic time-dependent salt-wedge regime. Such assumptions can certainly not be directly assessed from the present or former dataset, and would require prospective scenarios with dedicated numerical modelling to be further discussed. The potential changes on estuarine salinity structure might have significant consequences on biogeochemical processes controlled by mixing, residence time and water properties. Such issues should obviously not only concern the Adour system and call for a more extensive assessment of the impact of artificialisation and urbanisation of estuarine systems on the physical processes controlling the hydrodynamics and finally affecting the entire ecosystem.

The question arises then on the role of estuary engineering (channelisation and dredging) on the absence of observed ETM in the lower reach of the estuary, in particular when compared to other tidal estuaries. First, the width reduction at the estuary mouth certainly enhances the good flushing capacity of the lower Adour by reinforcing the ebbing currents. Such hypothesis might be impossible to confirm due to the lack of available data collected before those engineering works, a numerical study could be necessary to discuss further this issue. In addition, it is hypothesized that the artificialization of the river mouth tends to maintain a low marine sediment input, thus participating to the absence of ETM. At the river mouth, along the Northern jetty, a sand pit has been artificially created and maintained by dredging operations, in order to avoid sand accumulation in the estuary entrance under storm conditions. Dubranna's numerical study [11] highlighted that the transport of sediment from the coastal area into the estuary is strongly limited by this man-engineered retention pit. Grasso and al [23] have shown the important contribution of energetic wave conditions to the ETM mass, by sediment resuspension action. However, it has been demonstrated that both jetties located at the estuary entrance, efficiently protect the port against incoming swell and sea waves with a reduction factor of 85 % compared to the offshore wave energy [1]. All together, these interventions may also contribute to the absence of ETM in the Adour lower estuary. Nevertheless, the impacts of the artificialisation of the lower estuary on its hydrodynamics and sediment transport can not be quantified by the present study, and would require further investigations.

The plume generated by the brackish fresh waters flowing out the estuary is also influenced by the engineering works at the entrance of the estuary. As already mentioned the width reduction at the entrance of the estuary might be responsible for an intensification of the plume. In addition, the Northern jetty also affects the dispersion of the plume orienting the plume in the southwest direction. Such issue was not part of the scope of this study, however this could be the aim for additional research. Additional measurements upstream in the Adour estuary would be necessary to confirm such hypothesis.

5. Conclusion

This study aimed to investigate the hydro-sedimentary behaviour of the lower Adour estuary by means of field experiments. A series of hydrodynamical processes are documented through bottom-moored, hull-mounted and vertical profiling instrumentation. It has been shown that its functioning is strongly influenced by both river and tidal forcing, resulting in a wide range of density stratification. The stratification variations show different time scales : from flood to ebb tides, from neap to spring tides, even from dry to wet seasons. It has been demonstrated that stratification is strengthened during the flood tide and weakened during the ebb tide. During low river discharge, neap tides promote stable salt-wedge in the lower estuary, while spring tides allow full flushing of the salt-wedge. On the other hand, wet season has a tendency to constrain the salt-wedge in a thin bottom layer, enhancing the vertical stratification. This strong variability in the flow structure has a huge influence on the flushing capacity of the estuary.

The tidal evolution of the gradient of Richardson number has revealed the straight influence of the salinity structure on the turbulent mixing. Flood tide is generally associated with reduced turbulence production and stable stratification, while ebb tide is characterised by strong turbulent mixing. Through stratification and mixing characteristics of the Adour estuary, a recent classification scheme has been applied to compare it to others salt-wedge estuaries. Based on the Geyer and MacCready classification [21], the Adour estuary varies from salt-wedge to partially mixed estuary.

Density effects, salt-wedge displacement and the competition between stratification and mixing processes have a strong impact on the suspended matter displacement : longitudinal convergence at the salt tip, sinking of particles due to stratification induced turbulence damping, and re-suspension due to the salt-wedge passing. However, both major mechanisms associated with ETM generation have not been observed in the lower estuary : tidal asymmetry and residual estuarine circulation.

Acknowledgments

This study was sponsored by the EC2CO PANACHE program (CNRS INSU) and the MICROPOLIT project (European Regional Development Fund (ERDF) and Adour-Garonne Water Agency). The port of Bayonne, the Gladys group, MIO and EPOC supported the experimentation. We are grateful to all the contributors involved in this experiment, in particular to Stéphane Gubert whose efforts were essential to the deployment and Nagib Bhairy for Minibat operations.

[1] Florian Bellafont, Denis Morichon, Volker Roeber, Gaël André, and Stéphane Abadie. Infragravity period oscillations in a channel harbor near a river mouth. Coastal Engineering Proceedings, 1(36):8, 2018.

[2] Brière, C., 2005. Etude de l'hydrodynamique d'une zone côtière anthropisée: l'embouchure de l'adour et les plages adjacentes d'anglet. Ph.D. thesis, Pau.

[3] Bruce, L. C., Cook, P. L., Teakle, I., Hipsey, M. R., 2014. Hydrodynamic controls on oxygen dynamics in a riverine salt wedge estuary, the yarra river estuary, australia. Hydrology and Earth System Sciences 18 (4), 1397–1411.

[4] Burchard, H., Baumert, H., 1998. The formation of estuarine turbidity maxima due to density effects in the salt wedge. a hydrodynamic process study. Journal of Physical Oceanography 28 (2), 309–321.

[5] Burchard, H., Hetland, R. D., 2010. Quantifying the contributions of tidal straining and gravitational circulation to residual circulation in periodically stratified tidal estuaries. Journal of Physical Oceanography 40 (6), 1243–1262.

[6] Burchard, H., Schuttelaars, H. M., Ralston, D. K., 2018. Sediment trapping in estuaries. Annual review of marine science 10, 371–395.

[7] Cameron, W., Pritchard, D., 1963. Estuaries. in 'the sea, vol. 2'.(ed. mn hill.) pp. 306–324.

[8] Dailloux, D., 2008. Video measurements of the Adour plume dynamic and its surface water optical characteristics. Ph.D. thesis, Université de Pau et des Pays de l'Adour.

[9] de Nijs, M. A., Pietrzak, J. D., 2012. Saltwater intrusion and etm dynamics in a tidally-energetic stratified estuary. Ocean Modelling 49, 60–85.

[10] de Nijs, M. A., Winterwerp, J. C., Pietrzak, J. D., 2010. The effects of the internal flow structure on spm entrapment in the rotterdam waterway. Journal of Physical Oceanography 40 (11), 2357–2380.

[11] Dubranna, J., 2007. Etude des échanges sédimentaires entre l'embouchure de l'adour et les plages adjacentes d'anglet. Ph.D. thesis, Pau.

[12] Duinker, J., Hillebrand, M. T. J., Nolting, R., Wellershaus, S., Jacobsen, N. K., 1980. The river varde å: processes affecting the behaviour of metals and organochlorines during estuarine mixing. Netherlands Journal of Sea Research 14 (3-4), 237–267.

[13] Dyer, K., 1974. The salt balance in stratified estuaries. Estuarine and coastal marine science 2 (3), 273–281.

[14] Dyer, K., 1991. Circulation and mixing in stratified estuaries. Marine Chemistry 32 (2-4), 111–120.

[15] Dyer, K., Christie, M., Manning, A., 2004. The effects of suspended sediment on turbulence within an estuarine turbidity maximum. Estuarine, Coastal and Shelf Science 59 (2), 237–248.

[16] Dyer, K., Ramamoorthy, K., 1969. Salinity and water circulation in the vellar estuary. Limnology and Oceanography 14 (1), 4–15.

[17] Geyer, W., 2010. Estuarine salinity structure and circulation. Contemporary issues in estuarine physics, 12–26.

[18] Geyer, W. R., 1993. The importance of suppression of turbulence by stratification on the estuarine turbidity maximum. Estuaries 16 (1), 113–125.

[19] Geyer, W. R., Farmer, D. M., 1989. Tide-induced variation of the dynamics of a salt wedge estuary. Journal of Physical Oceanography 19 (8), 1060–1072.

[20] Geyer, W. R., Trowbridge, J. H., Bowen, M. M., 2000. The dynamics of a partially mixed estuary. Journal of Physical Oceanography 30 (8), 2035–2048.

[21] Geyer, W. R., MacCready, P., 2014. The estuarine circulation. Annual Review of Fluid Mechanics 46, 175–197.

[22] Glangeaud, L., 1938. Transport et sédimentation dans l'estuaire et à l'embouchure de la gironde. caractères pétrographiques des formations fluviatiles, saumâtres, littorales et néritiques. Bulletin de la Societe Geologique de France, Paris 7 (5), 599–630.

[23] Grasso, F., Verney, R., Le Hir, P., Thouvenin, B., Schulz, E., Kervella, Y., 2018. Suspended sediment dynamics in the macrotidal seine estuary (france): 1. numerical modeling of turbidity maximum dynamics. Journal of Geophysical Research: Oceans 123, 558–577.

[24] Hansen, D. V., Rattray, M., 1966. New dimensions in estuary classification. Limnology and Oceanography 11 (3), 319–326.

[25] Ibañez, C., Pont, D., Prat, N., 1997. Characterization of the ebre and rhone estuaries: A basis for defining and classifying salt-wedge estuaries. Limnology and Oceanography 42 (1), 89–101.

[26] Jalón-Rojas, I., Schmidt, S., Sottolichio, A., Bertier, C., 2016. Tracking the turbidity maximum zone in the loire estuary (france) based on a long-term, high-resolution and high-frequency monitoring network. Continental Shelf Research 117, 1 – 11.

[27] Jay, D. A., Orton, P. M., Chisholm, T., Wilson, D. J., Fain, A. M., 2007. Particle trapping in stratified estuaries: Application to observations. Estuaries and Coasts 30 (6), 1106–1125.

[28] Jouanneau, J.-M., Weber, O., Champilou, N., Cirac, P., Muxika, I., Borja, A., Pascual, A., Rodríguez-Lázaro, J., Donard, O., 2008. Recent sedimentary study of the shelf of the basque country. Journal of Marine Systems 72 (1-4), 397–406.

[29] Kemp, W., Testa, J., Conley, D., Gilbert, D., Hagy, J., 2009. Temporal responses of coastal hypoxia to nutrient loading and physical controls. Biogeosciences 6 (12), 2985–3008.

[30] Kostaschuk, R., Luternauer, J., 1989. The role of the salt-wedge in sediment resuspension and deposition: Fraser river estuary, canada. Journal of Coastal Research, 93–101.

[31] Lacy, J. R., Stacey, M. T., Burau, J. R., Monismith, S. G., 2003. Interaction of lateral baroclinic forcing and turbulence in an estuary. Journal of Geophysical Research: Oceans 108 (C3).

[32] Lerczak, J. A., Rockwell Geyer, W., 2004. Modeling the lateral circulation in straight, stratified estuaries. Journal of Physical Oceanography 34 (6), 1410–1428.

[33] Li, L., Wu, H., Liu, J. T., Zhu, J., 2014. Sediment transport induced by the advection of a moving salt wedge in the changjiang estuary. Journal of Coastal Research 31 (3), 671–679.

[34] Lu, Y., Lueck, R. G., 1999. Using a broadband adcp in a tidal channel. part ii: Turbulence. Journal of Atmospheric and Oceanic Technology 16 (11), 1568–1579.

[35] Nezu, I., Rodi, W., 1986. Open-channel flow measurements with a laser doppler anemometer. Journal of Hydraulic Engineering 112 (5), 335–355.

[36] Olabarrieta, M., Geyer, W. R., Coco, G., Friedrichs, C. T., Cao, Z., 2018. Effects of density-driven flows on the long-term morphodynamic evolution of funnel-shaped estuaries. Journal of Geophysical Research: Earth Surface 123 (11), 2901–2924.

[37] Petus, C., 2009. Qualité des eaux côtières du Sud du Golfe de Gascogne par télédétection spatiale. Ph.D. thesis, Université de Pau et des Pays de l'Adour.

[38] Point, D., Bareille, G., Amouroux, D., Etcheber, H., Donard, O. F., 2007. Reactivity, interactions and transport of trace elements, organic carbon and particulate material in a mountain range river system (adour river, france). Journal of Environmental Monitoring 9 (2), 157–167.

[39] Pritchard, D. W., 1952. Salinity distribution and circulation in the chesapeake bay estuarine system. Journal of Marine Research 11 (2), 106–123.

[40] Ralston, D. K., Geyer, W. R., Lerczak, J. A., 2008. Subtidal salinity and velocity in the hudson river estuary: Observations and modeling. Journal of Physical Oceanography 38 (4), 753–770.

[41] Ralston, D. K., Geyer, W. R., Lerczak, J. A., 2010. Structure, variability, and salt flux in a strongly forced salt wedge estuary. Journal of Geophysical Research: Oceans 115 (C6).

[42] Sahin, C., Verney, R., Sheremet, A., Voulgaris, G., 2017. Acoustic backscatter by suspended cohesive sediments: Field observations, seine estuary, france. Continental Shelf Research 134, 39 – 51.

[43] Scully, M. E., Friedrichs, C., Brubaker, J., 2005. Control of estuarine stratification and mixing by wind-induced straining of the estuarine density field. Estuaries 28 (3), 321–326.

[44] Scully, M. E., Geyer, W. R., 2012. The role of advection, straining, and mixing on the tidal variability of estuarine stratification. Journal of Physical Oceanography 42 (5), 855–868.

[45] Scully, M. E., Geyer, W. R., Lerczak, J. A., 2009. The influence of lateral advection on the residual estuarine circulation: A numerical modeling study of the hudson river estuary. Journal of Physical Oceanography 39 (1), 107–124.

[46] Simpson, J., Williams, E., Brasseur, L., Brubaker, J., 2005. The impact of tidal straining on the cycle of turbulence in a partially stratified estuary. Continental Shelf Research 25 (1), 51–64.

[47] Sous, D., Defontaine, S., Morichon, D., Bhairy, N., Lanceleur, L., Monperrus, M., 2018. Turbulence measurements in a stratified man-controlled estuary : The adour case. 16th International Symposium on Oceanography of the Bay of Biscay.

[48] Stacey, M. T., Brennan, M. L., Burau, J. R., Monismith, S. G., 2010. The tidally averaged momentum balance in a partially and periodically stratified estuary. Journal of Physical Oceanography 40 (11), 2418–2434.

[49] Stacey, M. T., Burau, J. R., Monismith, S. G., 2001. Creation of residual flows in a partially stratified estuary. Journal of Geophysical Research: Oceans 106 (C8), 17013–17037.

[50] Stacey, M. T., Ralston, D. K., 2005. The scaling and structure of the estuarine bottom boundary layer. Journal of Physical Oceanography 35 (1), 55–71.

[51] Toublanc, F., Brenon, I., Coulombier, T., Moine, O. L., 2015. Fortnightly tidal asymmetry inversions and perspectives on sediment dynamics in a macrotidal estuary (charente, france). Continental Shelf Research 94, 42 – 54.

[52] Toublanc, F., Brenon, I., Coulombier, T., 2016. Formation and structure of the turbidity maximum in the macrotidal charente estuary (france): Influence of fluvial and tidal forcing. Estuarine, Coastal and Shelf Science 169, 1–14.

[53] Turner, J. S., 1979. Buoyancy effects in fluids. Cambridge University Press.

[54] Uittenbogaard, R., 1995. The importance of internal waves for mixing in a stratified estuarine tidal flow. Ph.D. thesis, PhD thesis, Delfl University of Technology.

[55] Uncles, R., Stephens, J., Smith, R., 2002. The dependence of estuarine turbidity on tidal intrusion length, tidal range and residence time. Continental Shelf Research 22 (11-13), 1835–1856.

[56] Valle-Levinson, A., 2008. Density-driven exchange flow in terms of the kelvin and ekman numbers. Journal of Geophysical Research: Oceans 113 (C4).

[57] van Maanen, B., Sottolichio, A., 2018. Hydro- and sediment dynamics in the gironde estuary (france): Sensitivity to seasonal variations in river inflow and sea level rise. Continental Shelf Research 165, 37 – 50.

[58] Wellershaus, S., 1981. Turbidity maximum and mud shoaling in the weser estuary. Archiv fur Hydrobiologie 92 (2).

[59] West, J., Oduyemi, K., Shiono, K., 1991. Some observations on the effect of vertical density gradients on estuarine turbulent transport processes. Estuarine, Coastal and Shelf Science 32 (4), 365–383.

[60] Williams, E., Simpson, J. H., 2004. Uncertainties in estimates of reynolds stress and tke production rate using the adcp variance method. Journal of Atmospheric and Oceanic Technology 21 (2), 347–357.

[61] Winterwerp, J., 2001. Stratification effects by cohesive and noncohesive sediment. Journal of Geophysical Research: Oceans 106 (C10), 22559–22574.

- The first extensive study of the lower Adour estuary.

- The observations demonstrates a very high variability of the salinity structure, which has never been reported in the literature.

- No ETM has been identified in the present experimental conditions.

- The specific dynamics of the Adour estuary is discussed with respect to the roles of tide, river discharge and human engineering.

Sophie Defontaine
LMAP
Université de Pau et des Pays de l'Adour
France
sophie.defontaine@univ-pau.fr
+33 6 95 90 30 97

October the 7th, 2019

To whom it may concern,

On the behalf of all co-authors, I hereby declare to have no conflict of interest.

Sophie Defontaine